Scientia Iranica, Vol. 15, No. 3, pp 315–322
© Sharif University of Technology, June 2008

SCIENTIA
IRANICA

Research Note

Free Water Surface Oscillations in a Closed Rectangular Basin with Internal Barriers

A.R. Kabiri-Samani* and B. Ataie-Ashtiani[1]

Thee enclosed basin has certain natural frequencies of seiche, depending on the geometry of the water boundaries and the bathymetry of water depths. Therefore, the variation in the water surface at a point becomes irregular, as caused by the combination of several natural frequencies, which may be considered as the superposition of sinusoidal frequency components of different amplitude. This paper is mainly concerned with the motion of an incompressible irrotational fluid in a closed rectangular basin with internal impervious barriers. An analytical solution is presented for predicting the characteristic of generated waves in these types of basin. The equations of free water surface oscillations and its boundary conditions are reduced to a system of linear equations, which is solved by applying the small amplitude water wave theory. The flow potential, wave amplitude, flow patterns and the natural period of waves generated in the basin with impervious internal barriers are found, based on the basin geometry. It is shown that the natural period of the basin is strongly dependent on the location of the barriers and the size of the barrier opening.

INTRODUCTION

Standing waves are progressive waves reflected back on themselves and appear as alternating between troughs and crests at a fixed position. They occur in ocean basins, partly enclosed bays and seas and in estuaries. When a standing wave occurs, the surface alternately rises at one end and falls at the other end of the container (Figure 1). If different-sized containers are treated the same way, the period of oscillation increases as the length or depth of the container increase. Standing waves in natural basins are called seiches. Seiches can be generated by tectonic movements or winds.

The free oscillations are characteristic of the system and are independent of the exciting force, except for the initial magnitude. The restoring force is provided by gravity, which returns the fluid surface to its horizontal equilibrium position after it is displaced by wind or pressure variations. In lakes and harbours of small to medium size, the characteristic frequencies of free oscillations of the water surface (seiches) (Figure 1), depend only on the basin geometry. Like water sloshing in a bathtub, seiches are tide-like rises and drops in the coastal water levels of great lakes caused by prolonged strong winds that push the water toward one side of the lake, causing the water level to rise on the downwind side of the lake and to drop on the upwind side. When the wind stops, the water sloshes back and forth, with the near-shore water level rising and falling in decreasingly small amounts on both sides of the lake until it reaches equilibrium. They occur commonly in enclosed or partially enclosed basins and are usually the result of a sudden change, or a series of intermittent-periodic changes, in atmospheric pressure or wind velocity. The period of oscillation of a seiche depends on the causative force that sets the water basin in motion and the natural or free oscillating period of the basin.

Seiches can inflict damage. If the natural period

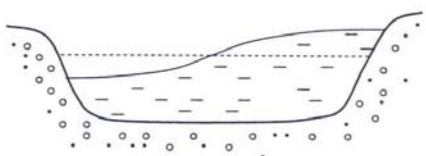

Figure 1. Formation of seiche.

*. *Corresponding Author, Department of Civil Engineering, Isfahan University of Technology, P.O. Box 84156, Isfahan, Iran. E-mail: akabiri@cc.iut.ac.ir*

1. *Department of Civil Engineering, Sharif University of Technology, P.O. Box 11155-9313, Tehran, Iran.*

of a moored ship matches that of a seiche, then, considerable motion will result in the moored ship. Seiches could damage structures along the coastline and create large vertical accelerations for offshore structures, such as boats, barges and floating piers. Shoreline flooding may be caused by storm surges or seiches, often occurring simultaneously with high waves.

A seiche is the free oscillation of the water in a closed or semi-enclosed basin at its natural period. Seiches are frequently observed in harbours, lakes, bays and in almost any distinct basin of moderate size. They may be caused by the passage of a pressure system over the basin or by the build-up and subsequent relaxation of a wind set-up in the basin. Following initiation of the seiche, the water sloshes back and forth until the oscillation is damped out by friction.

Seiches are not apparent in the main ocean basins, probably because there is no force sufficiently coordinated over the ocean to set a seiche in motion. If the natural period, or seiche period, is close to the period of one of the tidal species, the constituents of that species (diurnal or semidiurnal) will be amplified by resonance more than those of other species. The constituent closest to the seiche period will be amplified most of all, but the response is still a forced oscillation, whereas a seiche is a free oscillation. A variety of seiche periods may appear in the same water level record, because the main body of water may oscillate longitudinally or laterally at different periods. It may also oscillate, both in the open and closed mode, if the open end is somewhat restricted, and bays and harbours off the main body of water may oscillate locally at their particular seiche periods. Seiches generally have half-lives of only a few periods, but may be frequently regenerated. The largest amplitude seiches are usually found in shallow bodies of water of large horizontal extent, probably because the initiating wind set-up can be greater under these conditions. Seiching is the formation of standing waves in a water body, due to wave formation and subsequent reflections from the ends. These waves may be incited by earthquake motions, impulsive winds over the surface, or due to wave motions entering the basin. The various modes of seiching correspond to the natural frequency response of the water body. There are an infinite number of seiching modes possible, from the lowest (mode 1) to infinity. Realistically, the lower modes probably occur in nature, as frictional damping affects the higher modes preferentially (higher frequency). If the rectangular basin has significant width as well as length, both horizontal dimensions affect the natural period given in [1]:

$$T_{nm} = \left\{ \frac{2}{\sqrt{hg}} \left[\left(\frac{n}{a}\right)^2 + \left(\frac{m}{b}\right)^2 \right] \right\}^{-1/2}, \tag{1}$$

where T_{nm} is the natural free oscillation period, n and m are the modes of oscillation in longitudinal and lateral coordinates, respectively and a and b are the length and width of the rectangular basin. Forces of such wave motions have been attributed to tsunamis, surges or seiches, instability of wind, eddy trains caused by strong currents flowing across the harbour entrance, and surf-beat caused by long swell. However, the most studied are harbour oscillations caused by incident waves, which have typical periods of a few minutes. Due to strong winds or long wave energy, the water body of a harbour exhibits oscillatory resonant motions, which can damage moored ships and cause navigation hazards. A number of theoretical and numerical investigations of such resonant oscillations have been carried out, but most of them were limited to harbours with a constant depth connected to open sea. The free oscillation in closed rectangular and circular basins was analyzed by [2]. These solutions clarified the natural periods and modes of free surface oscillations related to these special configurations. McNown [3] studied the forced oscillation in a circular harbour connected to the open sea through a narrow mouth. Since the radiation effect was ruled out, the results showed a harbour resonance, as it does in a closed basin. The open-sea was important in allowing for the loss of energy radiated from a harbour (see [4,5]). The study of wave motion and its characteristics on a physical model of a small-boat harbour was undertaken in [6]. A weakly non-linear long internal wave in a closed basin was modelled by [7]. The free oscillation of water in a lake with an elliptic boundary was studied by [8]. Ishiguro [9] developed an analytical model for the oscillations of water in a bay or lake, using an electronic network and an electric analogue computer. The study of harbour resonance has been extended to take into account the effect of bottom friction by [10] and wave nonlinearity [11,12]. Ippen [1] studied free oscillation in a simple two-dimensional closed basin.

As an approach to an arbitrary-shaped harbour with a constant depth, a numerical model, using the boundary integral element method, was developed by [13,14]. For application to real depth-varying harbours, a hybrid finite element model is provided in [15] and a finite difference model is developed in [16]. A study of irregular wave incidence was undertaken by [17,18], viscous dissipation by [19] and porous breakwater by [20]. Lee and Park [21] developed a model for the prediction of harbour resonance, using the finite difference approach. Although the application of numerical models can be used for handling any complexities in this regard, the development of an analytical solution for practical cases would be very useful for the parametric study of the free oscillation phenomenon. In this work, an analytical solution for the calculation of free water surface oscillations in a rectangular basin with internal barriers will be presented. This analytical solution could be used to verify the accuracy of numerical models and calibrate experimental models, applicable in cases such as the construction of a causeway in lakes and an expansion plan for harbours. The water flow is considered as an ideal and irrotational flow. Therefore, the Laplace equation governs the velocity potential function of the flow domain. The free surface boundary condition is linearized to formulate a linear set of equations for solving the small amplitude water wave in the rectangular basin. The flow potential, wave amplitude and the natural period of waves generated in the basin with impervious internal barriers are found, based on the basin geometry. These parameters are presented for variations in basin and barrier geometries.

FREE OSCILLATION IN CLOSED BASINS WITH INTERNAL BARRIERS

Figure 2 illustrates a closed rectangular basin with the width of b, length of a and a constant depth of h, with two internal barriers of length b_u and b_d. The basin is divided into two semi-closed basins and it is assumed that the thickness of the barrier is small, in comparison with the other dimensions. There is an opening between the barriers that connects the sub-basins. To determine the natural periods of free water surface oscillations in this basin, an ideal flow field is considered. Therefore, the governing equation for the velocity potential function is the Laplace equation (Equation 2). Also, it is assumed that the amplitude of the water surface waves is small and, therefore, a linearized form of DFSBC can be applied.

$$\nabla^2 \Phi = 0. \tag{2}$$

The linearized kinematics and dynamic boundary conditions of the free surface for a left semi-closed basin

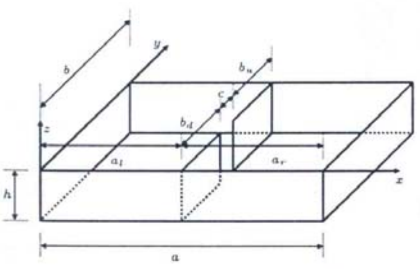

Figure 2. Schematic three-dimensional closed basin with internal barriers.

can be written as Equations 3-1 and 3-2:

$$\eta = \frac{1}{g}\frac{\partial \Phi}{\partial t} \quad \text{on} \quad z = 0, \tag{3-1}$$

$$-\frac{\partial \Phi}{\partial z} = \frac{\partial \eta}{\partial t} \quad \text{on} \quad z = \eta(x, y, t). \tag{3-2}$$

The bottom boundary condition is as follows:

$$w = -\frac{\partial \Phi}{\partial z} = 0 \quad \text{on} \quad z = -h. \tag{3-3}$$

The boundary conditions at the vicinity of barriers are as follows:

$$u = -\frac{\partial \Phi}{\partial x} = 0 \quad \text{on} \quad x = 0 \quad \text{for} \quad 0 \le y \le b, \tag{3-4}$$

$$u = -\frac{\partial \Phi}{\partial x} = 0 \quad \text{on} \quad x = a_l \quad \text{for} \quad 0 \le y \le b_d, \tag{3-5}$$

$$u = -\frac{\partial \Phi}{\partial x} = S_l \quad \text{on} \quad x = a_l \quad \text{for} \quad b_d \le y \le b_d + c, \tag{3-6}$$

$$u = -\frac{\partial \Phi}{\partial x} = 0 \quad \text{on} \quad x = a_l \quad \text{for} \quad b_d + c \le y \le b, \tag{3-7}$$

$$v = -\frac{\partial \Phi}{\partial y} = 0 \quad \text{on} \quad y = 0, b \quad \text{for} \quad 0 \le x \le a_l. \tag{3-8}$$

In a right semi-closed basin, the linearized boundary conditions can be written as follows:

$$\eta = \frac{1}{g}\frac{\partial \Phi}{\partial t} \quad \text{on} \quad z = 0, \tag{4-1}$$

$$-\frac{\partial \Phi}{\partial z} = \frac{\partial \eta}{\partial t} \quad \text{on} \quad z = \eta(x, y, t). \tag{4-2}$$

The bottom boundary condition is as follows:

$$w = -\frac{\partial \Phi}{\partial z} = 0 \quad \text{on} \quad z = -h. \tag{4-3}$$

The boundary conditions in the vicinity of the barriers are as follows:

$$u = -\frac{\partial \Phi}{\partial x} = 0 \quad \text{on} \quad x = 0 \quad \text{for} \quad 0 \le y \le b, \tag{4-4}$$

$$u = -\frac{\partial \Phi}{\partial x} = 0 \quad \text{on} \quad x = a_l \quad \text{for} \quad 0 \le y \le b_d, \tag{4-5}$$

$$u = -\frac{\partial \Phi}{\partial x} = S_r \quad \text{on} \quad x = a_l \quad \text{for} \quad b_d \le y \le b_d + c, \tag{4-6}$$

$$u = -\frac{\partial \Phi}{\partial x} = 0 \quad \text{on} \quad x = a_l \quad \text{for} \quad b_d + c \le y \le b, \tag{4-7}$$

$$v = -\frac{\partial \Phi}{\partial y} = 0 \quad \text{on} \quad y = 0, b \quad \text{for} \quad a_l \le x \le a. \tag{4-8}$$

To solve the differential equation, the method of the separation of variables is applied, hence:

$$\Phi = X(x).Y(y).Z(z).T(t). \tag{5}$$

Therefore:

$$\eta = \frac{1}{g}X(x).Y(y).Z(z).\frac{dT(t)}{dt}. \tag{6}$$

By substituting and dividing the domain in the y direction to three sub-domains, the solution is:

a) for $0 \leq y \leq b_d$

$$\Phi = \sum_{m=1}^{\infty}\sum_{n=1}^{\infty}\frac{gH}{2\sigma}\frac{\cosh k(h+z)}{\cosh kh}\cos\frac{n\pi x}{a_l}\cos\frac{m\pi y}{b}\sin\sigma t, \tag{7}$$

$$\eta = \sum_{m=1}^{\infty}\sum_{n=1}^{\infty}\frac{H}{2}\cos\frac{n\pi x}{a_l}\cos\frac{m\pi y}{b}\cos\sigma t, \tag{8}$$

b) $b_d \leq y \leq b_d + c$

Velocities S_l and S_r are equal and are evaluated by imposing the condition that the wave velocity at $x = a_l$ for a left semi-closed basin is the same as the wave velocity for a right semi-closed basin, at this point. Hence:

$$\Phi = \sum_{m=1}^{\infty}\sum_{n=1}^{\infty}\frac{gH}{2\sigma}\frac{\cosh k(h+z)}{\cosh kh}\cos\frac{n\pi x}{a}\cos\frac{m\pi y}{b}\sin\sigma t, \tag{9}$$

$$\eta = \sum_{m=1}^{\infty}\sum_{n=1}^{\infty}\frac{H}{2}\cos\frac{n\pi x}{a}\cos\frac{m\pi y}{b}\cos\sigma t, \tag{10}$$

c) $b_d + c \leq y \leq b$

The boundary conditions of this case are the same as those presented for Case a. By applying the boundary conditions for the right basin and dividing the domain in the y direction to three sub-domains, as below, the results will be given as:

a) $0 \leq y \leq b_d$

$$\Phi = \sum_{m=1}^{\infty}\sum_{n=1}^{\infty}\frac{gH}{2\sigma}\frac{\cosh k(h+z)}{\cosh kh}\left(\cos\frac{n\pi x}{a_r} + \tan\frac{n\pi a}{a_r}\sin\frac{n\pi x}{a_r}\right)\cos\frac{m\pi y}{b}\sin\sigma t, \tag{11}$$

$$\eta = \sum_{m=1}^{\infty}\sum_{n=1}^{\infty}\frac{H}{2}\left(\cos\frac{n\pi x}{a_r} + \tan\frac{n\pi a}{a_r}\sin\frac{n\pi x}{a_r}\right)\cos\frac{m\pi y}{b}\cos\sigma tm, \tag{12}$$

b) $b_d \leq y \leq b_d + c$

$$\Phi = \sum_{m=1}^{\infty}\sum_{n=1}^{\infty}\frac{gH}{2\sigma}\frac{\cosh k(h+z)}{\cosh kh}\cos\frac{n\pi x}{a}\cos\frac{m\pi y}{b}\sin\sigma t, \tag{13}$$

$$\eta = \sum_{m=1}^{\infty}\sum_{n=1}^{\infty}\frac{H}{2}\cos\frac{n\pi x}{a}\cos\frac{m\pi y}{b}\cos\sigma t, \tag{14}$$

c) $b_d + c \leq y \leq b$

The boundary conditions of this case are the same as those presented for Case a. For motion in both x and y directions, at a closed basin, which is divided into two semi-closed basins, the continuity for small amplitude water waves results from equating the change in flow in the two directions to the change in storage in the control volume (Figure 3).

$$h\left(\frac{\partial^2\Phi}{\partial x^2} + \frac{\partial^2\Phi}{\partial y^2}\right) + \frac{\partial\eta}{\partial t} = 0. \tag{15}$$

Substitution and simplification of results, for left and right basins, yields to:

$$T_s = \left\{\frac{2}{\sqrt{hg}}\left[\left(\frac{n}{a}\right)^2 + \left(\frac{m}{b}\right)^2\right]\right\}^{-1/2} \quad \text{for} \quad b_d \leq y \leq b_d + c,$$

$$T_{cl} = \left\{\frac{2}{\sqrt{hg}}\left[\left(\frac{n}{a_l}\right)^2 + \left(\frac{m}{b}\right)^2\right]\right\}^{-1/2} \quad \text{otherwise}, \tag{16}$$

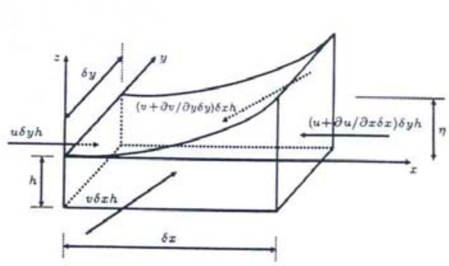

Figure 3. Selected control volume.

$$T_s = \left\{ \frac{2}{\sqrt{hg}} \left[\left(\frac{n}{a}\right)^2 + \left(\frac{m}{b}\right)^2 \right] \right\}^{-1/2}$$

for $b_d \leq y \leq b_d + c$,

$$T_{cr} = \left\{ \frac{2}{\sqrt{hg}} \left[\left(\frac{n}{a_r}\right)^2 + \left(\frac{m}{b}\right)^2 \right] \right\}^{-1/2} \quad \text{otherwise.} \tag{17}$$

RESULTS

In this section, the results of the analytical solution presented above, for a closed rectangular basin with internal barriers, are discussed. Figure 4 shows the variation of the normalized water level, η/H, versus x/a for various values of a_l/a. As shown, the wavelength decreases as the ratio of a_l/a increases. The results are the same as those for a simple closed basin without barriers under limiting conditions of a_l/a equals 0 and 1. Figure 5 illustrates the variation of the normalized water level, η/H, versus y/b for various values of c/b. The wavelength decreases as the values of c/b and b_u/b (or b_d/b) increase. The opening size, c, has a significant influence on the normalized water level (η/H) at various positions in the basin. For the limiting case of $c/b = 1$, the results are the same as those in the case of a simple basin. Also, for the case of $c/b = 0$, when there is no opening between barriers, the results are the same as those for a simple half basin. Increasing the value of b_u/b decreases the wavelength and its natural period, except under limiting conditions.

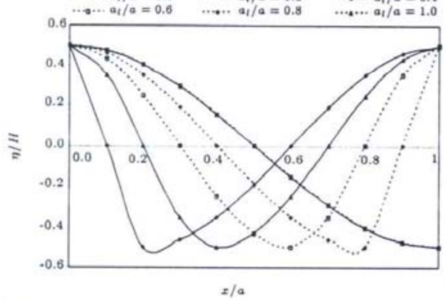

Figure 4. Variation of normalized water level versus x/a for various values of a_l/a.

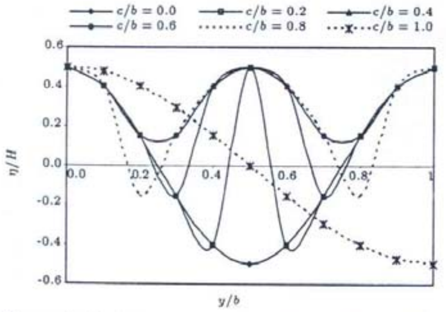

Figure 5. Variation of normalized water level versus y/b for various values of c/b, when $b_u = b_d$.

Figure 6 illustrates the variation of the non-dimensional parameter, a_n, defined as $a_n = (u\sigma/gH)a$, versus x/a for different a_l/a and mode $m = n = 1$. From this figure and the parameter, a_n, defined here, the horizontal velocity at the x coordinate is obtained, knowing the dimensions of the basin. As shown in this figure, the significant effect of a_l/a on the parameter, a_n, can be seen. Also, the results are symmetrical (the results of a_l/a and $1 - a_l/a$ are the same). The amplitude of variation of the velocity component, u, in an x direction, decreases as the ratio, a_l/a. increases. As shown, the increase in the value of a_l/a causes a decrease in a_n and u. Figure 7 shows the variation in the maximum values of a_n versus a_l/a. As shown, the increase in the value of a_l/a causes a decrease in a_n and u.

Figure 8 shows the variation of the non-dimensional parameter, b_n, defined as $b_n = (v\sigma/gH)b$, versus y/b, for different modes. From this figure and the parameter, b_n, defined here, the horizontal velocity at the y coordinate is obtained, knowing the dimensions of the basin. From this figure, the significance of the modes of oscillation on parameter b_n can be seen. As seen, an increase in the mode number causes an increase in the amplitude of the horizontal velocity (v).

As seen, an increase in the mode number causes an increase in the amplitude of the horizontal velocity

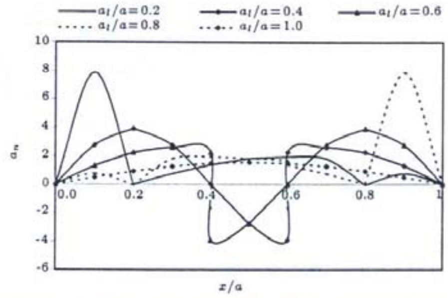

Figure 6. Variation of parameter $u\sigma a/(gH)$ by x/a for different a_l/a.

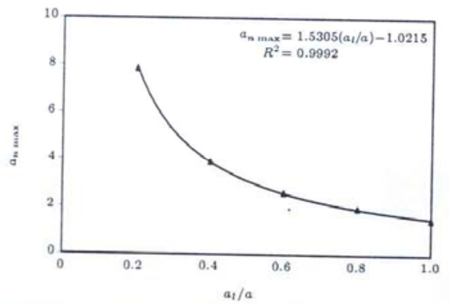

Figure 7. Variation of maximum values of parameter $u\sigma a/(gH)$ versus a_l/a.

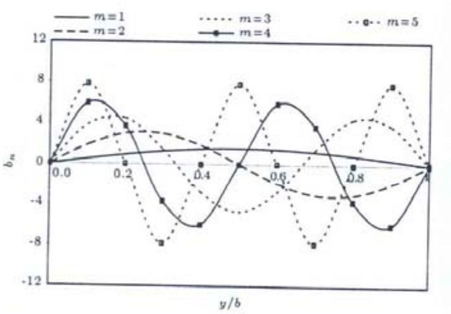

Figure 8. Variation of parameter $b_n = v\sigma b/(gH)$ versus y/b for different modes.

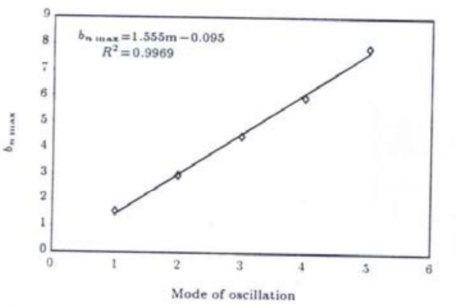

Figure 9. Variation of the maximum values of parameter $b_n = v\sigma b/(gH)$ versus different modes.

(v). This result clearly can be seen in Figure 9. In this figure, the variation of the maximum values of b_n, versus mode number, m, is presented.

Figure 10 shows the normalized natural period, T_{cl}/T_s (or T_{cr}/T_s), versus a_l/a (or a_r/a) for different values of b/a. As seen, an increase in the value of b/a

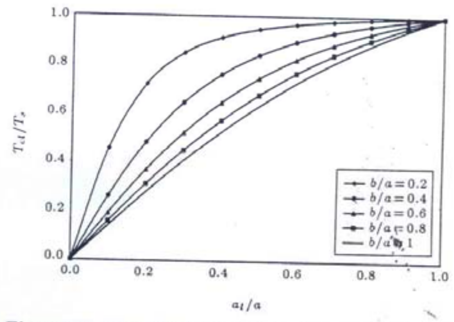

Figure 10. Normalized natural period of coupled basin to simple basin versus a_l/a or a_r/a for different b/a ratios and $m = n = 1$.

causes an increase in the natural period of the coupled basin. When the basin becomes square, the natural period becomes the greatest.

Figure 11 illustrates the variation of the dimensionless parameter, $S_n = T_c\sqrt{hg}/2b$, versus b/a_l, for different modes. From this figure, the natural modes by varying the position of the barrier. As seen, an increase in the value of b/a_l, decreases the non-dimensional parameter, defined above.

Figure 12 shows the normalized water level contours for different modes of a simple closed basin and a closed basin with an internal barrier, where $al/a = 0.5$ and $c/b = 0.2$, and a simple closed basin with an internal continual barrier, where $al/a = 0.5$ for different modes. These figures illustrate the differences of the flow pattern among these three cases. From these figures, the significant influence of internal barriers on the flow map, the wavelength and, more importantly, the natural frequency of free oscillation in the basin are shown.

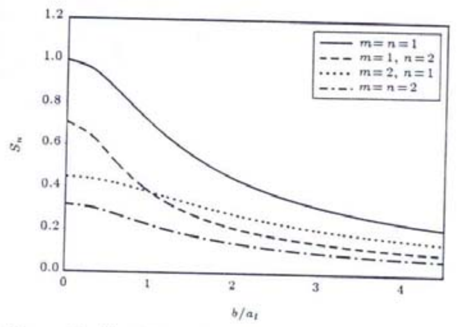

Figure 11. Non-dimensional parameter $T_c(hg)^{0.5}/(2b)$ variations by b/a_l.

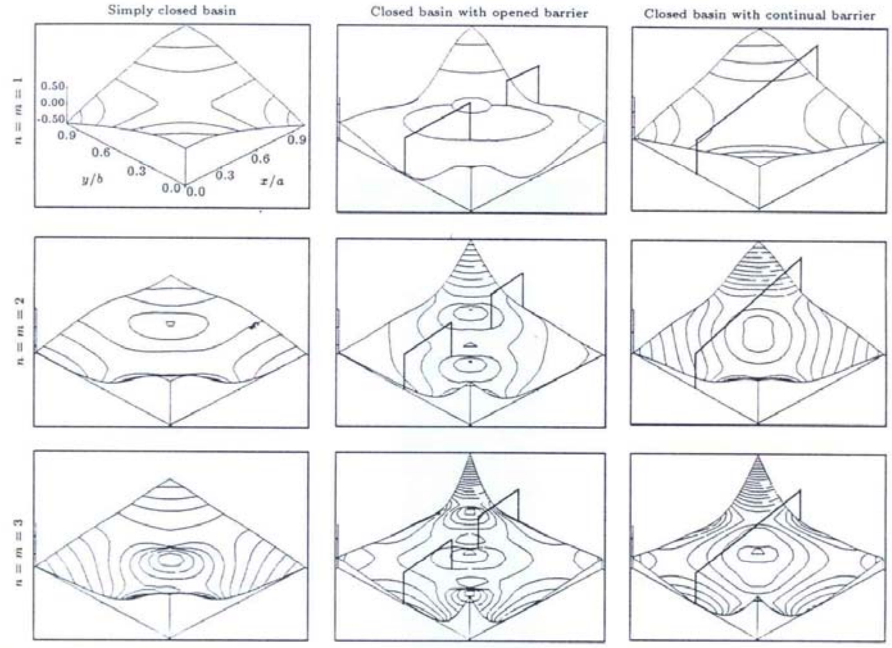

Figure 12. The normalized water level contours for closed simple basin and closed basin with internal barrier; $c = 0.2$ and $a_l = a_r$.

SUMMARY

An analytical solution for free surface oscillations in a rectangular basin with internal barriers was presented. The water flow was considered as an ideal flow. Therefore, the Laplace equation governs the velocity potential function of the flow domain. The free surface boundary condition was linearized to formulate a linear set of equation for solving the small amplitude water wave in the rectangular basin. The flow potential, wave amplitude and the natural period of waves generated in the basin with impervious internal barriers were found, based on the basin geometry. It was shown that barrier geometry significantly influences the flow map, wavelength and natural frequency of free water oscillation in the basin.

NOMENCLATURE

H	wave height
T_n	natural free oscillation period
T	the largest period
T_{cl}, T_{cr}	natural period for left and right semi basins, respectively
T_s	natural period of simple closed basin
S_n	non-dimensional parameter, defined as $S_n = T_c\sqrt{hg}/2b$
S_l, S_r	velocities in x direction at the station of the barrier opening for left and right semi basins, respectively
$X(x), Y(y)$	functions of x and y which demonstrate flow field or amplitude functions
$Z(z), T(t)$	functions of z and t, which demonstrate flow field or amplitude functions
a, b	dimensions of simple closed basin
a_l, a_r	dimensions of semi basins in x direction
a_n	defined as $a_n = (u\sigma/gH)a$
$a_{n\,\max}$	the maximum of a_n
b_u, b_d	the size of up and down barriers, respectively
b_n	defined as $b_n = (v\sigma/gH)b$
$b_{n\,\max}$	the maximum of b_n

c	the opening size
g	gravitational acceleration
h	water depth
k	wave number
l	length of closed basin along the axis
m, n	integers show the oscillation mode
t	time
u, v	velocity components in x and y directions
x, y, z	coordinates
η	water level (amplitude)
σ	wave frequency
Φ	velocity potential function

REFERENCES

1. Ippen, A.T., *Estuary and Coastal Hydrodynamics*, McGraw-Hill Inc., USA (1982).
2. Lamb, S.H., *Hydrodynamics*, University of Cambridge, 6th Ed. (1932).
3. McNown, J.C. "Waves transmission through porous structures", *Journal of Waterway Harbour and Coastal Engrg. Division., ASCE*, **100**(3), pp 169-188 (1952).
4. Ippen, A.T. and Goda, Y. "Wave induced oscillations in harbours: The solution of a rectangular harbour connected to the open sea", *Report No. 59*, Hydrodynamics Lab., MIT, Cambridge (1963).
5. Miles, J.W. and Munk, W.H. "Harbor Paradox", *Journal of Waterways, Harbors and Coastal Engrg. Division., ASCE*, **87**(3), pp 111-130 (1961).
6. Bottin, R.R. "Physical modelling of small-boat harbours: Design experience, lessons learned, and modelling guidelines", Technical Report (ADA258700), U.S. Army Engineer Waterways Experiment Station, Vicksburg, MS, USA (1992).
7. Horn, D.A., Imberger, J., Ivey, G.N. and Redekopp, L.G. "A weakly nonlinear model of long internal waves in closed basins", *Journal of Fluid Mechanics*, Cambridge University Press, **467**, pp 269-287 (2002).
8. Iida, F. "On the free oscillation of water in a lake of elliptic boundary", *Journal of the Oceanographical Society of Japan*, **21**(3), pp 103-108 (1965).
9. Ishiguro, S. "An analytical method for the oscillations of water in a bay or lake, using an electronic network and an electric analogue computer", *Journal of the Oceanographical Society of Japan*, **11**(4) pp 191-197 (1955).
10. Kostense, J.K., Meijer, K.L., Dinemans, M.W., Mynett, A.E. and Van Den Bosch, P. "Wave energy dissipation in arbitrarily shaped harbors of variable depth", *20th ICCE*, pp 436-437 (1986).
11. Lapelletier, T.G. and Raichlen, F. "Harbor oscillations induced by nonlinear transient long waves", *Journal of Waterway, Port, Coast and Ocean Engrg.*, **113**(4), pp 381-400 (1987).
12. Zhou, C.P. and Cheung, Y.K. and Lee, J.H.W. "Response in harbour due to incidence of second order low-frequency waves", *Wave Motion*, **13**, pp 167-184 (1991).
13. Hwang, L.S. and Tuck, E.O. "On the oscillation of harbors of arbitrary shape", *J. Fluid Mech.*, **42**, pp 447-464 (1970).
14. Lee, J.J. "Wave-induced oscillations in harbors of arbitrary shape", *J. Fluid Mech.*, **45**, pp 375-394 (1971).
15. Mei, C.C. and Chen, H.S. "Hybrid element method for water waves", *2nd Annual Symp. of Waterways, Harbors and Coastal Engrg. Div., ASCE*, **1**, pp 63-81 (1975).
16. Raichlen, F. and Naheer, E. "Wave induced oscillations of harbors with variable depth", *Proc. 15th ICCE., ASCE*, pp 3536-3556 (1976).
17. Goda, Y., *Random Seas and Design of Maritime Structure*, University of Tokyo Press, Tokyo, Japan (1985).
18. Ouellet, Y. and Theriault, T. "Wave grouping effect in irregular wave agitation in harbour", *Jour. Wtrway., Port, Coast and Ocean Engrg.*, **115**(3), pp 363-383 (1989).
19. Gember, M. "Modeling dissipation in harbor resonance", *Coastal Engrg.*, **10**, pp 211-252 (1986).
20. Yu, X. and Chwang, A.T. "Wave-induced oscillation in harbor with porous breakwaters", *Jour. Wtrway., Port, Coast and Ocean Engrg.*, **120**(2), pp 125-144 (1994).
21. Lee, J.L. and Park, C.S. "Prediction of harbor resonance by the finite difference approach", *Korean Society of Coastal and Ocean Eng.*, Asou University, Suwon, Korea (1998).